Biochemical Pharmacology 81 (2011) 412–424

Contents lists available at ScienceDirect

Biochemical Pharmacology

journal homepage: www.elsevier.com/locate/biochempharm

NFκB inhibitors induce cell death in glioblastomas

Alfeu Zanotto-Filho [a,*], Elizandra Braganhol [b], Rafael Schröder [a], Luís Henrique T. de Souza [a], Rodrigo J.S. Dalmolin [a], Matheus A. Bittencourt Pasquali [a], Daniel Pens Gelain [a], Ana Maria Oliveira Battastini [b], José Cláudio Fonseca Moreira [a]

[a] Centro de Estudos em Estresse Oxidativo, Departamento de Bioquímica, Universidade Federal do Rio Grande do Sul (UFRGS), Porto Alegre, Rio Grande do Sul, Brazil
[b] Laboratório de Enzimologia, Departamento de Bioquímica, Universidade Federal do Rio Grande do Sul (UFRGS), Porto Alegre, Rio Grande do Sul, Brazil

ARTICLE INFO

Article history:
Received 14 August 2010
Accepted 21 October 2010

Keywords:
NFκB
Glioblastoma
NFκB inhibitors
Apoptosis
Chemotherapy

ABSTRACT

Identification of novel target pathways in glioblastoma (GBM) remains critical due to poor prognosis, inefficient therapies and recurrence associated with these tumors. In this work, we evaluated the role of nuclear-factor-kappa-B (NFκB) in the growth of GBM cells, and the potential of NFκB inhibitors as antiglioma agents. NFκB pathway was found overstimulated in GBM cell lines and in tumor specimens compared to normal astrocytes and healthy brain tissues, respectively. Treatment of a panel of established GBM cell lines (U138MG, U87, U373 and C6) with pharmacological NFκB inhibitors (BAY117082, parthenolide, MG132, curcumin and arsenic trioxide) and NFκB-p65 siRNA markedly decreased the viability of GBMs as compared to inhibitors of other signaling pathways such as MAPKs (ERK, JNK and p38), PKC, EGFR and PI3K/Akt. In addition, NFκB inhibitors presented a low toxicity to normal astrocytes, indicating selectivity to cancerous cells. In GBMs, mitochondrial dysfunction (membrane depolarization, bcl-xL downregulation and cytochrome c release) and arrest in the G2/M phase were observed at the early steps of NFκB inhibitors treatment. These events preceded sub-G1 detection, apoptotic body formation and caspase-3 activation. Also, NFκB was found overstimulated in cisplatin-resistant C6 cells, and treatment of GBMs with NFκB inhibitors overcame cisplatin resistance besides potentiating the effects of the chemotherapeutics, cisplatin and doxorubicin. These findings support NFκB as a potential target to cell death induction in GBMs, and that the NFκB inhibitors may be considered for in vivo testing on animal models and possibly on GBM therapy.

1. Introduction

Glioblastoma (GBM) is an aggressive, invasive, and difficult to treat primary brain tumor. Standard therapy includes surgical resection, external beam radiation and chemotherapy, with no known curative therapy [1]. A number of dysregulated signaling cascades have been described in GBMs, including the MEK/ERK pathway, PLC/PKC pathway, and the PI3K/Akt pathway. Dysregulation of these pathways is driven by mutation, amplification, or overexpression of multiple genes such as PTEN, EGFR, PDGFR-a, p53, and mTOR [2–4]. Understanding these dysregulated pathways has provideded the basis for designing molecular targeted therapies as monoclonal antibodies against EGF, VEGF and PDGF receptors, as well as new combination therapies and drug delivery systems [4–6]. Despite these new treatment strategies, median survival has remained approximately 1 year for decades [1]. Thus, it is urgent to determine novel molecular targets in GBMs in order to develop more effective therapies and new therapeutic opportunities to patients.

Studies have compelling evidence that the transcription factor NFκB (Nuclear factor κB) plays a role in the control of oncogenesis, tumor progression and chemotherapy resistance of diverse types of malignances as lymphoma, leukemia, breast and ovarian cancers [7–11]. NFκB is formed by homo or heterodimers comprising members of the Rel family of proteins (p50/p105, p52/p100, p65, c-Rel and RelB) which form, upon non-stimulated conditions, a ternary and inactive cytoplasmic complex by interacting with inhibitory proteins of the IκB family. Upon stimulation by cytokines (TNF-alpha and IL1-beta), growth factors (EGF and PDGF), anticancer drugs (cisplatin, doxorubicin and vincristine) and other stressor stimuli, IκBs are phosphorylated by IKK (IκB kinase) proteins thus releasing the active NFκB, which translocates into nucleus and binds to DNA sequences in gene promoters. NFκB binding to DNA modulates the expression of a wide range of genes as that involved in inflammation (IL1-beta, IL-6, COX2, and TNF), apoptosis resistance (bcl-xL, cIAP1/2, XIAP, FLICE and survivin), cell

* Corresponding author at: Depto. Bioquímica (ICBS-UFRGS), Rua Ramiro Barcelos, 2600/Anexo, Porto Alegre CEP 90035-003, Rio Grande do Sul, Brazil. Tel.: +55 51 3308 5578; fax: +55 51 3308 5535.
E-mail address: alfeuzanotto@hotmail.com (A. Zanotto-Filho).

0006-2952/$ – see front matter © 2010 Elsevier Inc. All rights reserved.
doi:10.1016/j.bcp.2010.10.014

invasion (ICAM-1, VCAM-1, MMP2, MMP9), angiogenesis (VEGF), proliferation (cyclin D1, MYC) and metastasis (CXCR4 and TWIST) [7–12]. These groups of genes are directly related to tumor-associated phenomena suggesting NFκB as a potential target to cell death induction and chemosensitization in cancer [9,13–15].

Aberrant NFκB activity has been described in some types of cancer cells upon basal and following anticancer drugs treatments. Besides, constitutive NFκB up-regulation has been found in chemotherapy-resistant cell lines, which correlates with therapy failure [9,13,15–17]. In this context, studies have suggested that molecules with NFκB inhibitory properties are potential anticancer agents [9,15,17,18]. In this intent, researchers have blocking NFκB activity via IKK/NFκB inhibitors (as BAY117082, BAY117085, parthenolide, curcumin, arsenic trioxide and PDTC) or proteasome/NFκB inhibitors (PS-341 and MG132) in order to inhibit the growth of myeloma [10], leukemia [17,19], esophageal [14] and breast cancer cells [20]. Recently, analysis of brain tumor biopsies identified that NFκB and its target genes are overexpressed in GBM and astrocytoma tumors compared to normal brain tissues [21,22]. In addition, a positive correlation between NFκB activation and poor GBM prognosis was reported, suggesting that the known role of NFκB as a survival factor in other cancers could also be considered in GBMs [23]. Taken into account the aforementioned, this study was undertaken in order to determine the role of NFκB in GBM growth, and the selectivity, apoptotic potential and chemosensitizing activity of the NFκB inhibitors BAY117082, parthenolide, curcumin, arsenic trioxide, MG132, and p65 small-interfering RNA in GBM cell lines.

2. Materials and methods

2.1. Reagents and antibodies

BAY117082 ((E)3-[(4-methylphenyl)-sulfonyl]-2-propenenitrile); MG132 (Z-Leu-Leu-Leu-CHO), curcumin, arsenic trioxide, propidium iodide, Hepes, CHAPS, dithiothreitol, EDTA, trypsin, MTT (3-(4,5-dimethyl)-2,5-diphenyl tetrazolium bromide), Nonidet-P40, spermin tetrahydrochloride, RNAse A and culture analytical grade reagents were purchased from Sigma Chemical Co. (St. Louis, MO, USA). Anti-NFκB p65 rabbit polyclonal antibody and anti-Lamin B were from Santa Cruz Biotechnologies; anti-β-actin was from Cell Signaling Technology; SP600129 was from Promega Corporation (Madison, USA). SB203580 were from Merck Biosciences (Darmstadt, Germany). Anti-cytochrome c antibody was from BD PharMingen (San Diego, USA). Parthenolide, LY294002, UO126 and Gö6983 were from Biomol International (Plymouth Meeting, PA). PD158780 was from Tocris Bioscience (MO, USA). Electrophoresis/immunoblotting reagents were from Bio-Rad Laboratories (Hercules, CA, USA).

2.2. Cell cultures

The rat (C6) and human (U138MG, U87 and U373) malignant GBM cell lines were obtained from American Type Culture Collection (Rockville, MD, USA). Cells were grown and maintained in low glucose Dulbecco's modified Eagle's medium (DMEM; Gibco BRL, Carlsbad, USA), containing 0.1% Fungizone, 100 U/l gentamicin and supplemented with 10% fetal bovine serum. Cells were kept at 37 °C in a humidified atmosphere with 5% CO_2. Primary astrocyte cultures were prepared as previously described [24]. Briefly, cortex of newborn Wistar rats (1–2 days old) was removed and mechanically dissociated in a Ca^{2+} and Mg^{2+} free balanced salt solution (137 mmol/L NaCl, 5.36 mmol/L KCl, 0.27 mmol/L Na_2HPO_4, 1.1 mmol/L KH_2PO_4, 6.1 mmol/L glucose; pH 7.4). After centrifugation at 1000 rpm (5 min), the pellet was resuspended in DMEM supplemented with 10% FBS. The cells (2×10^5) were plated in 48 multi-well plates pretreated with poly-L-lysine. After 4 h platting, plates were gently shaken, cells were washed with PBS, and medium was changed to remove neuron and microglia contaminants. Cultures were allowed to grow by 20–25 days (100% confluence). Medium was replaced every 4 days.

2.3. MTT and LDH assays

Dehydrogenase-dependent MTT reduction (MTT assay) and lactate dehydrogenase release into culture medium from cells with losses in membrane integrity (LDH assay) were used as an estimative of cell viability [15,17]. Cells were plated in 96-well plates (10^4/well) and treated after to reach 60–70% confluence as detailed in Section 3. At the end of incubation, MTT and LDH assays were performed. Lactate dehydrogenase (LDH) release into culture medium was determined by fluorescent assay kit (CytoTox 96-NonRadioactive Cytotoxicity Assay, Promega) as recommended by the manufacturer. Qualitative morphology of the cell cultures was also evaluated by light microscopy (Nikon Eclipse TE 300), and the cell cultures were classified as: normal (cells with unaltered morphology and normal density); low-density (cell with normal morphology and low-density/lower number in plates); and dead cells (altered cellular/nuclear morphology, cytoplasm vacuolization, and presence of detached cells).

2.4. Propidium iodide incorporation and staining of chromatin

For the determination of propidium iodide (PI) uptake in cells with losses in membrane integrity, treated cells were incubated with 2 μg/mL PI in complete medium for 1 h. PI fluorescence was excited at 515–560 nm using an inverted microscope (Nikon Eclipse TE 300) fitted with a standard rhodamine filter. Representative microphotographs (at least 5/well) were collected [25]. For the detection of the morphological alterations in chromatin (condensation and fragmentation) and apoptotic body formation, cells were fixed in methanol/acetone (1:1) for 5 min and washed with PBS (3 times). Then, chromatin was stained with PI (0.5 μg/mL, 10 min) followed by fluorescent microscopy (Nikon Eclipse TE 300).

2.5. Cell cycle analysis

For cell cycle analysis, cells were trypsinized, centrifuged and resuspended in a lysis buffer (3.5 mmol/L trisodium citrate, 0.1% (v/v) Nonidet P-40, 0.5 mmol/L Tris–HCl, 1.2 mg/mL spermine tetrahydrochloride, 5 μg/mL RNAse, 5 mmol/L EDTA, 1 μg/mL propidium iodide, pH 7.6), vortexed and incubated for at least 10 min on ice for cell lysis. DNA content was determined by flow cytometry. Ten thousand events were counted per sample. FACS analyses were performed in the CellQuest Pro software (BD Biosciences, CA) [17].

2.6. Caspase-3 activity

Caspase-3 activity was assessed in agreement with CASP3F Fluorimetric kit (Sigma, St. Louis/MI). Treated cells were harvested and incubated in a lysis buffer (50 mmol/L Hepes, 5 mmol/L CHAPS and 5 mmol/L dithiothreitol, pH 7.4) for 20 min in ice. Later, extracts were clarified by centrifugation at 13,000 × *g* (15 min, 4 °C). Supernatants were collected and proteins were measured by Bradford method. For assays, 150 μg proteins were mixed with 200 μL of the assay buffer (20 mmol/L Hepes, 0.1% CHAPS, 5 mmol/L dithiothreitol, 2 mmol/L EDTA, pH 7.4) plus 20 μM Ac-DEVD-AMC (Acetyl-Asp-Glu-Val-Asp-7-amido-4-methylcoumarin), a caspase-3 specific substrate. Caspase-3-mediated substrate cleavage was monitored for 1 h (37 °C) in a fluorimetric reader (excitation 360 nm/emission 460 nm) [17].

2.7. Cellular fractionation

For nuclear extracts preparation, cells (~5×10^6, 70–80% confluence) were washed with cold phosphate-buffered saline (PBS) and suspended in 0.4 mL hypotonic lysis buffer (10 mmol/L HEPES (pH 7.9), 1.5 mmol/L $MgCl_2$, 10 mmol/L KCl, 0.5 mmol/L phenylmethylsulfonyl fluoride, 0.5 mmol/L dithiothreitol plus protease inhibitor cocktail (Roche)) for 15 min. Cells were then lysed with 12.5 μL 10% Nonidet P-40. The homogenate was centrifuged (13,000 × *g*, 30 s), and supernatants containing the cytoplasmic extracts (fraction 1) were stored at −80 °C. The nuclear pellet was resuspended in 100 μL ice-cold hypertonic extraction buffer (10 mmol/L HEPES (pH 7.9), 0.42 M NaCl, 1.5 mmol/L $MgCl_2$, 10 mmol/L KCl, 0.5 mmol/L phenylmethylsulfonyl fluoride, 1 mmol/L dithiothreitol plus protease inhibitors). After 40 min of intermittent mixing, extracts were centrifuged (13,000 × *g*, 10 min, 4 °C), and supernatants containing nuclear proteins were secured. To detect cytochrome c release from mitochondria, mitochondria-free cytoplasmic extracts were obtained from centrifugation of the cytoplasmic extracts (fraction 1) at 14,000 × *g*, 20 min, 4 °C. The resultant supernatant (mitochondria-free cytosolic proteins) and mitochondrial pellets were stored at −80 °C. The protein content was measured by the Bradford method [17,26].

2.8. NFκB-p65 ELISA assay for the determination of NFκB activity

A total of 10 μg of nuclear extracts was used to determine NFκB activation (NFκB p65 ELISA kit, Stressgen/Assays designs) as per the manufacturer protocols. This ELISA-based chemiluminescent detection method rapidly detects activated NFκB complex binding (p65 detection) to a plate-adhered NFκB consensus oligonucleotide sequence. Kit-provided nuclear extracts prepared from TNF-stimulated Hela cells were used as a positive control for NFκB activation. To demonstrate assay specificity, a 50-fold excess of an NFκB consensus oligonucleotide was used as competitor to block NFκB binding. In addition, a mutated consensus NFκB oligonucleotide (which do not binds NFκB) is provided for the determination of binding reactions' specificity [15].

2.9. siRNA knockdown of the NFκB protein p65

The Silencer® Select Validated NFκB-p65 siRNA (siRNA ID# s11914; Ambion® Inc.) was transfected using the siPORT™ NeoFX™ Transfection Agent (Ambion®, Applied Biosystems Inc.) in agreement with manufacturer's protocol. U138MG cells were transfected with 50–100 nM of NFκB-p65 siRNA by reverse transfection and then incubated for 72 h in Opti-MEM to allow knockdown of the p65 protein, which was confirmed by Western blotting. Silencer® Select Negative Control#1 siRNA containing scrambled sequences was used as negative control.

2.10. Immunocytochemistry for NFκB p65 localization

For the determination of subcellular distribution of NFκB, cells were cultured up to 60–70% confluence in 12-well plates. After a brief washing with PBS, cells were fixed in 4% (v/v) formaldehyde in PBS for 20 min at room temperature. Fixed cells were rinsed three times with PBS and then permeabilized with 0.5% Triton X-100 in PBS for 15 min at room temperature. After that, cells were washed with PBS and blocked with 5% BSA for 1 h. At the end of incubation, cells were incubated with rabbit anti-p65 polyclonal antibody (1:500; overnight at 4 °C), and then incubated with a goat anti-rabbit IgG Alexa 594-conjugated antibody (1:500) for 2 h at room temperature. Cells were visualized in a fluorescence microscope (Nikon Eclipse TE 300) [27].

2.11. Western blotting

Proteins (20 μg) were separated by SDS-PAGE on 10% (w/v) acrylamide, 0.275% (w/v) bisacrylamide gels, and electrotransfered onto nitrocellulose membranes. Membranes were incubated in TBS-T (20 mmol/L Tris–HCl, pH 7.5, 137 mmol/L NaCl, 0.05% (v/v) Tween 20) containing 1% (w/v) non-fat milk powder for 1 h at room temperature. Subsequently, the membranes were incubated for 12 h with the appropriate primary antibody (dilution range 1:500–1:1000), rinsed with TBS-T, and exposed to horseradish peroxidase-linked anti-IgG antibodies for 2 h at room temperature. Chemiluminescent bands were detected using X-ray films, and densitometry analyses were performed using Image-J® software.

2.12. Mitochondria membrane potential (JC-1 assay)

For the determination of the mitochondrial membrane potential (MMP), treated cells (5×10^5) were incubated for 30 min at 37 °C with the lipophilic cationic probe JC-1 (5,5′,6,6′-tetrachloro-1,1′,3,3′ tetraethylbenzimidazolcarbocyanine iodide, 2 μg/mL). After that, JC-1-loaded cells were centrifuged and washed once with PBS. Cells were transferred to a 96-well plate and assayed in a fluorescence plate reader with the following settings: excitation at 485 nm, emission at 540 and 590 nm, and cutoff at 530 nm (SpectraMax M2, Molecular Devices, USA). $\Delta\Psi_m$ was calculated using the ratio of 590 nm (J-aggregates)/540 nm (monomeric form) [28].

2.13. Clonogenic potential

Exponentially growing cells (1×10^6) were plated in Petri plates overnight, and then incubated for 36 h with either vehicle or NFκB inhibitors. After treatments, the medium containing NFκB inhibitors was replaced by a new medium without the tested compounds, and remaining cells were maintained for additional 24 h to growth. Survival cells were gently washed and trypsinized, and viability was assessed by Trypan Blue staining. Viable cells (10^4 cells) were re-plated in 6-well plates and maintained for additional 6 days in complete culture medium. Cell growth was estimated by colony counting followed by MTT assay [15,29]. The percentage of colony forming efficiency was calculated in relation to values of untreated cells.

2.14. Soft agar colony assay

Cells (1×10^5) were resuspended in 2 mL DMEM supplemented with 15% FBS and mixed with 1 mL of 1.6% agarose (final conditions: 0.53% agarose and 10% FBS) at 37 °C. Cell suspensions were placed on top of a base layer comprising 2 mL of DMEM with 10% FBS and 0.8% agarose in each well of a six-well plate. Cells were then covered with 2 mL of complete media and, after 3 days, a new medium containing NFκB inhibitors was added. Media containing treatments or vehicle were replaced every 72 h. At the end of 9 days, MTT (1 mg/mL) was added to the cultures and the number of colonies was scored using a microscope [15].

2.15. NFκB gene/protein-association network and landscape analysis of gene expression

The NFκB gene/protein interaction network was constructed by associating 46 NFκB-induced and cancer-related human genes involved in antiapoptotic defenses (14 genes), proliferation (8 genes), inflammation (10 genes) and invasion/metastasis/angiogenesis (9 genes), besides the NFκB subunits (5 genes). Genes were selected based on current literature [7,11,30,31]. Briefly, the network is generated using STRING database [32] with input

options 'databases', 'experiments', 'textmining' and 0.700 confidence level. STRING integrates different curate and public databases containing information on direct and indirect functional protein–protein associations/interactions. Each protein is identified according to both HUGO Gene Symbol [33] and Ensembl Peptide ID [34]. The selected gene list is applied in the STRING database and the links (interaction strength) between two different genes are saved in data files, which were handled in the Medusa software [35].

After being constructed, the NFκB gene network was analyzed by the ViaComplex software, which was previously developed and validated in our laboratory [36]. ViaComplex plots the gene expression activity over the Medusa network topology. To do this, ViaComplex overlaps functional information (micro-array expression data) with interaction information (the NFκB network) and distributes the microarray signal according to the coordinates of the network objects (i.e. nodes and links) thus constructing 3D landscape modules. Microarray expression data were collected from the international repository Gene Expression Omnibus (GEO-accession number: GSE12657; Platform: GPL8300, Affymetrix), and were composed of 20 human gliomas – 7 GBM; 7 oligodendroglioma (ODG); 6 pilocytic astrocytoma (PA) – which were compared to 5 healthy brain (HB) control biopsies. For each gene, means of each gene expression in each glioma type was plotted over the expression of the same gene in healthy brains (HB), and landscapes were constructed. Gene expression in GBM, ODG and PA versus HB tissues was statistically analyzed by *t*-test, and *p*-values were calculated.

2.16. Statistical analysis

Data are expressed as means ± SD and were analyzed by one-way ANOVA followed by Duncan's post hoc test. Differences were considered significant at $p < 0.05$.

3. Results

3.1. NFκB as potential target to cell death induction in GBMs

Initially, we treated U138MG and C6 cells with inhibitors of some signaling pathways which are described as dysregulated in GBMs and other cancers [2–4]. Inhibitors of PI3K/Akt (LY294002, wortmannin), EGFR (PD158780), MEK/ERK1/2 (UO126), JNK1/2 (SP600129), p38 MAPK (SB203580), PKC (Gö6983), proteasome/NFκB (MG132) and IKK/NFκB (BAY117082) were tested at different concentrations (1–60 μM) based on the literature range and manufacturer instructions, which describe IC_{50} values < 20 μM for all the tested drugs. At the end of 36 h incubation, only the compounds with NFκB inhibitory activity (BAY11082 and MG132) promoted significant decreases in GBM viability compared to inhibitors of other tested signaling pathways (Table 1). NFκB inhibitors reduced viability as assessed by MTT assays, increased LDH release in culture medium and altered cell

Table 1
Effect of cell signaling pathway inhibitors on viability of GBMs.

Treatments	Viability (MTT assay)		LDH	Qualitative morphology
	C6	U138MG	U138MG	U138MG
Untreated	100 ± 4	100 ± 6	100 ± 11	Normal
UO126 (30 μM)	93 ± 15	96 ± 7	92 ± 10	Normal
SP600129 (30 μM)	103 ± 11	101 ± 4	109 ± 6	Normal
SB203580 (30 μM)	98 ± 10	95 ± 6	101 ± 5	Normal
LY294002 (50 μM)	64 ± 17*	74 ± 4*	108 ± 9	Low-density
Wortmannin (10 μM)	85 ± 5*	75 ± 9*	102 ± 4	Low-density
Gö6983 (30 μM)	96 ± 9	95 ± 7	111 ± 7	Normal
PD158780 (50 μM)	99 ± 4	96 ± 5	112 ± 6	Normal
MG132 (5 μM)	21 ± 14*	23 ± 17*	223 ± 38*	Dead cells
BAY117082 (30 μM)	15 ± 6*	36 ± 9*	554 ± 39*	Dead cells

C6 and U138MG cells were treated for 36 h with well-established pathway inhibitors and MTT, LDH and qualitative microscopy assays were performed. Experiments were repeated three times ($n = 3$) in triplicate, and data were expressed in mean ± SD.
* Different from untreated cells in each type of assay.

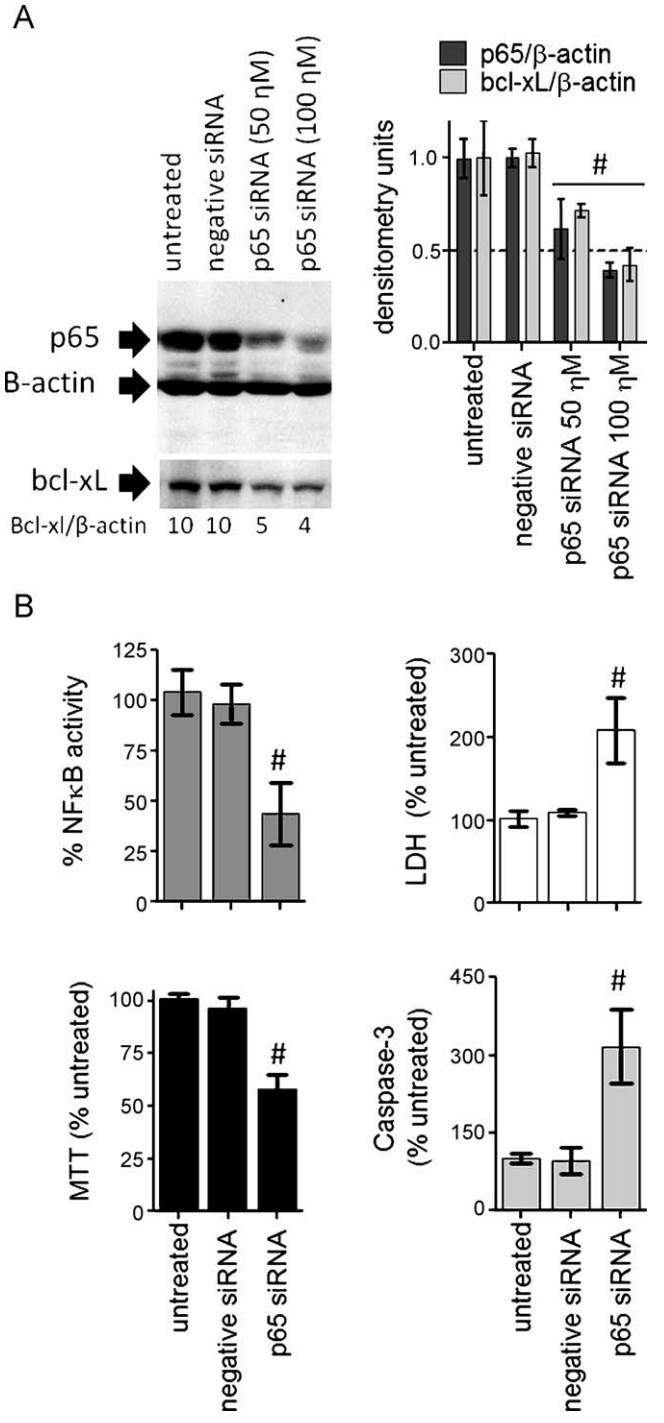

Fig. 1. NFκB-p65 knockdown induces apoptotic cell death in U138MG cells. (A) Representative immunoblotting and densitometry for the determination of p65 knockdown efficiency and bcl-xL levels. U138MG cells were incubated for 72 h with 50 or 100 nM p65 siRNA and cellular extracts were collected. (B) MTT, LDH, caspase-3 activity and NFκB ELISA assays in p65-downregulated U138MG cells. For these experiments, cells were incubated for 72 h with 100 nM p65 siRNA. All experiments were performed in triplicate. Graphs were expressed in mean ± SD. #Different from untreated cells from its respective assay.

morphology as indicative of cell death (Table 1 and Fig. 3A). Although the PI3K/Akt inhibitors LY294002 and wortmannin decreased MTT values, the absence of both LDH release and alterations in cell morphology, besides the observed decreases in cell density, suggests that PI3K/Akt inhibition affected GBM cell proliferation, but not induced cell death (Table 1). Thus, we decided to perform our further experiments with NFκB inhibitors. MAPKs (JNK, p38 and ERK1/2), EGFR, PKC inhibitors did not present cytotoxic effects up to 60 μM (data not shown). As control, we also performed Western blotting for the detection of the basal levels of phosphorylated forms of MAPKs (JNK, p38 and ERK1/2), Akt and PKC substrates; ELISA assay was performed to detect NFκB activity. Of the tested pathways, only PI3K/Akt and NFκB were detected at basal/non-stimulated conditions (data not shown).

3.2. NFκB-p65 member knockdown induces apoptosis in GBM cells

To assess the specific role of NFκB in GBM cells survival, we performed siRNA experiments to knockdown the NFκB p65 member in human U138MG cells. Immunoblotting confirmed the p65 siRNA protocol efficiency to down p65 protein after 72 h incubation with siRNAs (Fig. 1A). p65 knockdown was accompanied by the inhibition of NFκB DNA-binding activity (Fig 1B, upper left panel) and by decreases in bcl-xL protein levels (Fig. 1A), a classical antiapoptotic NFκB target gene product [7,11,13], thus confirming the effect of p65 knockdown upon NFκB signaling. As a consequence of NFκB downregulation, cell viability decreased by 45–55% as assessed by MTT. Detection of increased LDH release into culture medium and caspase-3 activation confirmed cell death induction in p65-silenced cells (Fig. 1B).

3.3. NFκB is up-regulated in GBMs compared to non-tumor astrocytes

NFκB overstimulation has been observed in several cancer cell lines as a consequence of cytokine overproduction, mutations, cell cycle dysregulation and apoptosis resistance [8,15,19]. In C6 and U138MG, we found a 5–10-fold increase in the basal activity of NFκB compared to primary astrocytes as assessed by NFκB p65 ELISA (Fig. 2A). LPS-treated cells (0.5 μg/mL, 3 h) were used as positive control for NFκB activation. Assay specificity was assessed by the incubation of nuclear extracts with a 50-fold excess of an unlabeled oligonucleotide containing the NFκB consensus sequence, which completely inhibited the constitutive NFκB binding (C6 + 50X lane). In addition, mutated NFκB oligonucleotides did not alter the constitutive NFκB activity confirming the specificity of binding reactions (C6 + mut lane, Fig. 2A). Determination of total and nuclear p65 immunocontent confirmed that a significant fraction of p65 is found in nuclear compartment of GBM cells whereas astrocytes expressed predominantly cytoplasmic/latent p65 (Fig. 2B). In C6 cells, nuclear accumulation of p65 was more accentuated. Detection of Lamin B and absence of Adenine Nucleotide Translocator (ANT) were assessed to confirm the purity of nuclear extracts (Fig. 2B). Immunocytochemistry to p65 confirmed the accumulation of p65 in nuclear compartment of C6 cells, corroborating with the Western blotting data shown in Fig. 2C.

3.4. Landscape analysis of NFκB target genes expression in human gliomas

Besides in vitro detection of NFκB in GBM cell lines (Fig. 2), we decided to test whether the cancer-related NFκB target genes are

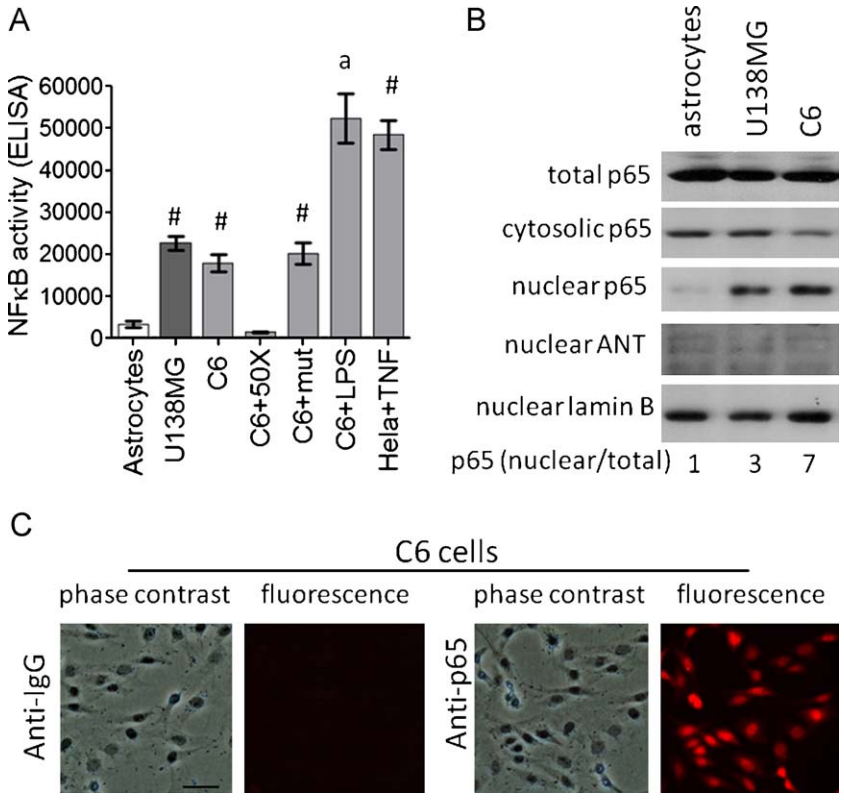

Fig. 2. NFκB is up-regulated in GBMs compared to primary astrocytes. (A) Basal NFκB activation in nuclear extracts isolated from C6, U138MG and astrocytes as assessed by ELISA. (B) Representative Western blotting showing p65 protein compartmentalization in C6, U138MG and astrocytes. (C) Representative immunocytochemistry for p65 in C6 cells (20× magnification). In these experiments, cells were maintained in basal conditions (complete culture medium for 48 h) and nuclear and cytoplasmic extracts were isolated to detect NFκB activity, p65 immunocontent, or fixed for immunocytochemistry. Lamin B and ANT levels in nuclear extracts were used as controls of nuclear extract purity. [#]Different from astrocytes; [a]different from its respective untreated cell line ($p < 0.05$, ANOVA, $n = 3$).

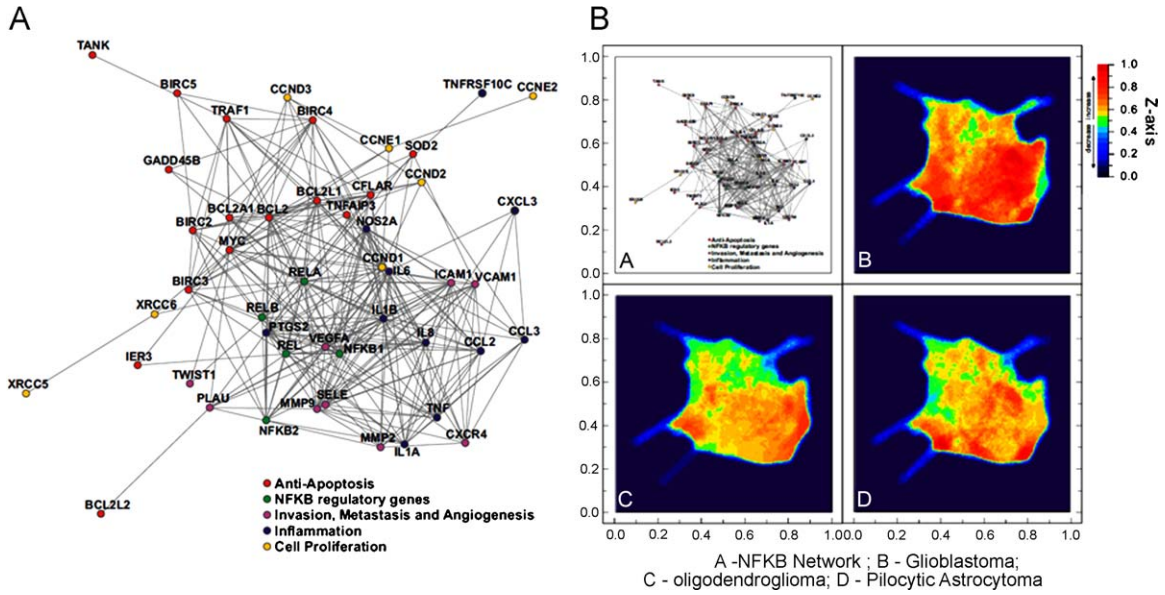

Fig. 3. Landscape analysis of NFκB gene/protein interaction networks in gliomas. (A) NFκB-target gene interaction network. Network was generated using STRING database. Gene symbol was collected from HUGO, and interactions were handled in Medusa software for network construction. (B) Landscape analysis of NFκB network gene expression in clinical specimens of glioblastoma (B panel), oligodendroglioma (C panel) and pilocytic astrocytoma (D panel). Gene expression in different types of glioma was plotted against gene expression in healthy brain tissues, and *Z*-axis for relative gene expression was constructed using the ViaComplex software.

modulated in human GBM biopsies. We collected microarray experiments containing the gene expression pattern for different glioma grades [pilocytic astrocytoma (PA), oligodendroglioma (ODG) and glioblastoma multiforme (GBM)], besides health brain (HB) biopsies. First, we constructed an NFκB gene/protein interactions network (Fig. 3A), which was subsequently analyzed by ViaComplex software as described in Section 2. ViaComplex landscapes were constructed by plotting gene expression values of each different glioma types over HB gene expression. ViaComplex-constructed *Z*-axis gives the relative gene expression in gliomas over gene expression in healthy brains. Fig. 3B shows that NFκB gene interaction network was up-regulated in the 3 grades of

Table 2
Normalized expression of NFκB-target genes in healthy brains (HB), glioblastoma (GBM), oligodendroglioma (ODG) and pilocytic astrocytoma (PA) specimens.

Gene function	Invasion/angiogenesis/metastasis								Antiapoptosis				Inflammation	
	MMP9	MMP2	CXCR4	ICAM1	PLAU	VCAM1	VCAM2	VEGFA	SOD2	MYC	A20	IER3	CCL2	IL8
HB1	102	130	304	106	102	148	136	92	70	118	177	112	320	97
HB2	109	114	61	107	73	38	89	88	10	107	121	65	30	139
HB6	99	72	44	98	44	117	91	98	251	60	71	112	20	95
HB7	95	93	63	93	54	136	91	113	394	71	67	81	27	85
HB11	94	91	28	96	226	61	93	108	102	143	67	131	100	85
GBM1	256	149	1525	3512	882	5629	2755	2320	1400	506	1077	372	825	103
GBM4	383	221	277	92	4776	305	144	1176	22	1051	140	8	12	124
GBM6	98	301	448	1866	2702	9004	5019	180	841	257	232	92	777	76
GBM7	11,212	214	2392	23,316	5237	6452	4164	19,305	2078	1235	2619	1334	2800	74,989
GBM10	2951	129	2805	2531	190	6931	3034	6413	916	175	960	315	297	965
GBM12	4490	256	911	141	484	363	312	7849	111	180	282	261	1219	434
GBM13	36,827	296	1021	17,323	11,240	4757	2020	3791	921	490	1331	916	2858	59,217
p-Value	0.017	0.005	0.005	0.048	0.005	0.003	0.006	0.016	0.049	0.040	0.010	0.035	0.073	0.103
ODG1	102	129	577	80	46	324	425	543	81	1081	177	452	174	120
ODG3	107	225	647	110	73	1213	656	43	87	2559	121	542	554	149
ODG4	222	163	50	115	91	91	104	162	9	189	71	95	153	185
ODG5	117	149	27	121	74	62	224	223	99	3196	67	371	194	1761
ODG6	109	247	226	118	101	425	298	150	9	1269	67	221	201	146
ODG7	104	144	257	120	124	2069	2062	88	34	419	97	509	783	128
ODG8	77	112	252	76	48	270	255	207	224	181	105	49	45	60
p-Value	0.190	0.020	0.340	0.270	0.930	0.073	0.0092	0.220	0.270	0.0025	0.930	0.036	0.073	0.310
PA1	88	220	1278	112	1556	215	78	156	14	298	805	619	333	97
PA2	88	139	1492	472	183	715	375	126	135	143	729	292	243	90
PA3	126	123	2938	1011	4179	65	93	376	106	875	1016	479	276	90
PA5	100	137	453	3318	14345	59	137	174	92	899	150	459	179	82
PA6	93	132	1049	5745	4805	81	75	228	43	181	781	421	342	63
PA12	86	342	1153	85	372	62	75	249	12	257	835	98	159	68
p-Value	0.25	0.069	0.007	0.082	0.0087	0.790	0.850	0.017	0.530	0.010	0.135	0.006	0.033	0.123

Mean of expression of each gene in HB was plotted as 100% (±SD) and the respective gene expression in glioma (GBM, ODG or PA) specimens was compared to these values and percentage was calculated. Percentage and *p*-values were expressed. Other details are provided in Section 2.

glioma, although GBM samples presented the higher levels of gene expression for the NFκB-regulated genes as evidenced by the red colors in *Z*-axis plots. Grouping NFκB genes by biological functions, we found that 8/9 (89%) of the selected NFκB-regulated genes described as involved in angiogenesis, invasiveness and metastasis (VEGFA, MMP2, MMP9, ICAM1, VCAM1, VCAM2, CXCR4 and PLAU) and in antiapoptotic defenses (MYC, SOD2, A20/TNFAIP3 and IER3) were markedly up-regulated in GBM patients (up to 64-fold increases, $p < 0.05$) compared to HB tissues (Table 2). Increases in the inflammatory IL8 and CCL2 mRNAs ($p < 0.1$) also were observed in GBM patients. Gene expression for NFκB subunits (RELA, REL, NFKB2 and RELB, except NFKB1) was comparable to HB, suggesting that NFκB is regulated at the activation level, not at subunit expression (data not shown). Besides increasing in GBMs, MYC, CCL2 and IER3 genes also were increased in the lower grades of glioma (ODG and PA; Table 2).

Table 3
IC_{50} levels of NFκB inhibitors in a panel of GBMs and in primary astrocytes.

Treatments	IC_{50} (μM)				
	U138MG	C6	U87	U373	Astrocytes
BAY117082	17 ± 5*	15 ± 6*	9.5 ± 7*	15 ± 4*	75 ± 8
Parthenolide	22 ± 5*	29 ± 6*	17 ± 4*	13 ± 5*	186 ± 10
MG132	2.5 ± 0.8*	3.9 ± 0.7*	5 ± 1*	2.7 ± 1*	35 ± 5
Curcumin	23 ± 5*	25 ± 4*	20 ± 6*	21 ± 3*	135 ± 12
Arsenic trioxide	4.6 ± 2*	4.2 ± 1.5*	3.6 ± 2*	5 ± 1*	18 ± 2

Cells (U138MG, U87, C6, U373 and astrocytes) were treated for 36 h with different concentrations of NFκB signaling inhibitors (BAY117082, curcumin, parthenolide, MG132 and arsenic trioxide; 1–200 μM) and cell viability was determined by MTT assay. Experiments were repeated three times ($n = 3$) in triplicate, and data were expressed in mean ± SD.

* Different from untreated cells, and from its respective astrocytic IC_{50} value ($p < 0.05$).

3.5. Pharmacological inhibitors of NFκB selectively induce cell death in GBMs

Data from Table 1, and Figs. 2 and 3, indicate that NFκB could be a potential target pathway to cell death induction in GBMs. Thus, we decided to test the cytotoxic effect of some NFκB pathway inhibitors such as BAY117082, parthenolide, arsenic trioxide, MG132 and curcumin in a panel of GBM cell lines. In parallel, primary astrocyte cultures were treated in order to evaluate the drug selectivity to cancer cells. GBMs and astrocytes were incubated with different concentrations of NFκB inhibitors for 36 h, and MTT assays were performed. Results show that astrocytes were less sensitive to NFκB inhibitors than GBM cell lines, indicating selectivity of NFκB inhibitors to tumor cells (Table 3). For BAY117082, parthenolide, MG132, curcumin and arsenic trioxide, the IC_{50} values in MTT assay were, respectively, at least 4.4, 6.4, 7, 4 and 3.6-fold lower in the GBM cell lines compared to astrocytes as shown in Table 3. Thus, for further experiments, we used ~IC_{50} concentrations for NFκB inhibitors (17 μM BAY117082; 25 μM curcumin; 3 μM MG132; 4 μM arsenic trioxide; 25 μM parthenolide) and C6/U138MG cell lines. To determine whether the effects of pharmacological NFκB inhibitors are directly NFκB related, indirectly related to NFκB inhibition, or have nothing to do with NFκB, we evaluated different concentrations of the compounds on NFκB activity and on cell viability as shown in Table 4. Correlations between NFκB inhibition and decreases in cell viability were calculated (Table 4). Data showed that pharmacological agent-induced NFκB inhibition significantly correlated with decreases in cell viability of both C6 and U138MG cells. As control, we also determined that inhibitors of the signaling pathways which were previously tested in Table 1 did not affect NFκB activity (Table 5). Taken together, data from Tables 1, 4 and 5 suggest that the antiglioma effects of the tested compounds were directly related to their NFκB inhibitory activity.

3.6. NFκB inhibitors induce anchorage-independent cell death and reduce the clonogenic potential in GBMs

Results from clonogenic survival assay showed that 36 h treatment with NFκB inhibitors followed by 6-day washout significantly decreased the clonogenic proliferation in GBMs, suggesting that the antiglioma effects of NFκB inhibition were long-term thus remaining after drug withdrawal (Fig. 4B). In addition, data from soft agar experiments showed that NFκB

Table 4
NFκB inhibition is correlated with decreases in cell viability in GBMs.

Treatments	Concentration (μM)	NFκB activity (%, mean ± SD)		% cell viability (MTT assay)		Correlation (r^2) Viability × NFκB	
		C6	U138MG	C6	U138MG	C6	U138MG
Untreated	0	100 ± 11	100 ± 12	100 ± 7	100 ± 6		
BAY117082	5	85 ± 14	87 ± 15	86 ± 6	95 ± 7	0.931#	0.952#
	25	47 ± 15*	35 ± 10*	17 ± 9*	37 ± 12*		
	50	13 ± 9*	17 ± 5*	5 ± 3*	15 ± 4*		
Parthenolide	5	92 ± 13	88 ± 12	80 ± 12	91 ± 5	0.846#	0.971#
	25	24 ± 11*	34 ± 21*	54 ± 5*	48 ± 7*		
	50	15 ± 14*	20 ± 9*	15 ± 6*	19 ± 4*		
MG132	1	72 ± 9*	79 ± 6*	66 ± 11*	71 ± 6*	0.974#	0.981#
	5	37 ± 13*	21 ± 17*	26 ± 5*	23 ± 7*		
	10	12 ± 6*	14 ± 8*	15 ± 7*	11 ± 5*		
Curcumin	5	93 ± 8	99 ± 10	94 ± 5	89 ± 4	0.978#	0.962#
	25	47 ± 12*	49 ± 22*	46 ± 7*	40 ± 9*		
	50	24 ± 13*	11 ± 7*	9 ± 8*	21 ± 11*		
Arsenic	1	82 ± 7*	91 ± 12	95 ± 9	92 ± 7	0.954#	0.975#
	5	25 ± 13*	29 ± 18*	41 ± 7*	45 ± 4*		
	10	18 ± 6*	24 ± 9*	17 ± 11*	27 ± 9*		

C6 and U138MG cells were treated with different concentrations of BAY117082, curcumin, parthenolide, MG132 or arsenic trioxide. MTT was performed after 36 h treatment; ELISA assays for NFκB-p65 DNA-binding activity were performed in nuclear extracts isolated from 6 h-treated GBMs. Cell viability and NFκB inhibition were expressed as percentage compared to untreated cells. *R* squared (R^2) was calculated using GraphPad Prism software®. Experiments were repeated three times ($n = 3$) in duplicate; data were expressed as mean ± SD.

* Different from untreated cells.

\# Positive correlation.

inhibitor-induced cell death was independent of cell anchorage since NFκB inhibitors decreased cell colony formation in soft agar (Fig. 4C). At the end of 36 h treatment with NFκB inhibitors, we also observed significant alterations in cell morphology, which were accompanied by PI uptake, cell detachment and LDH release as indicative of cell death (Fig. 4A). PI uptake did not occur in all cells with morphological changes, suggesting that morphological alterations preceded the losses in cell membrane integrity. These effects suggest a programmed mechanism of cell death induction by NFκB inhibitors thus stimulating us to evaluate apoptotic markers (Fig. 4A).

3.7. NFκB inhibitors cell cycle arrest and apoptosis in GBMs

PI staining of chromatin showed that NFκB inhibitors induced chromatin condensation and apoptotic body formation in U138MG cells (Fig. 5A). The results were similar in C6 cells (data not shown). Determination of caspase-3 activity showed that all the tested NFκB inhibitors promoted caspase-3 activation in C6 whereas only MG132 and arsenic trioxide increased caspase-3 activity in the p53/PTEN mutant U138MG, suggesting that apoptosis can be caspase-3 dependent or independent depending on cell type and on NFκB inhibitor (Fig. 5B). Analysis of cell cycle distribution evidenced that, after 18 h treatment, NFκB inhibitors caused accumulation of cells in the G2/M phase of the cell cycle followed by the formation of sub-G1 apoptotic cells at 36 h, suggesting that arrest in G2/M phase preceded apoptosis (Fig. 5C).

3.8. Mitochondrial dysfunction precedes apoptosis in NFκB inhibitor-treated cells

We also evaluated the mitochondrial function in NFκB inhibitor-treated GBMs. In time-effect experiments, we determined that NFκB inhibitors promoted an early decrease in MMP (JC-1 assay) which was observed between 8 and 16 h treatment whereas cell membrane integrity (PI uptake assay) only decreased at later time points (24 h treatment) (Fig. 6A). It suggests that mitochondrial dysfunction occurred at the early steps of NFκB inhibitor-induced

Table 5
Effect of MAPKs, EGFR, PKC and PI3K/Akt inhibitors on NFκB activity.

Treatments	Concentration (μM)	NFκB activity (%, mean ± SD)
Untreated	0	100 ± 8
UO126	10	110 ± 11
	30	112 ± 22
SP600129	10	106 ± 12
	30	114 ± 7
SB203508	10	88 ± 22
	30	95 ± 16
PD158780	10	90 ± 8
	30	106 ± 14
LY294002	10	88 ± 11
	30	86 ± 21
Gö6983	10	112 ± 13
	30	93 ± 9
Wortmannin	1	89 ± 15
	10	93 ± 11
BAY117082	30	39 ± 12*

C6 cells were treated with different concentrations of pharmacological inhibitors of MEK/ERK (UO126), JNK1/2 (SP600129), p38 (SB203508), EGFR (PD158780), PI3K/Akt (LY294002 and wortmannin) and PKC (Gö6983). BAY117082 was used as control for NFκB inhibition. ELISA assays for NFκB-p65 DNA-binding activity were performed in nuclear extracts isolated from 6 h-treated cells. NFκB activity was expressed as percentage compared to untreated cells (mean ± SD). Experiments were performed in triplicate.
* Different from untreated cells ($p < 0.05$).

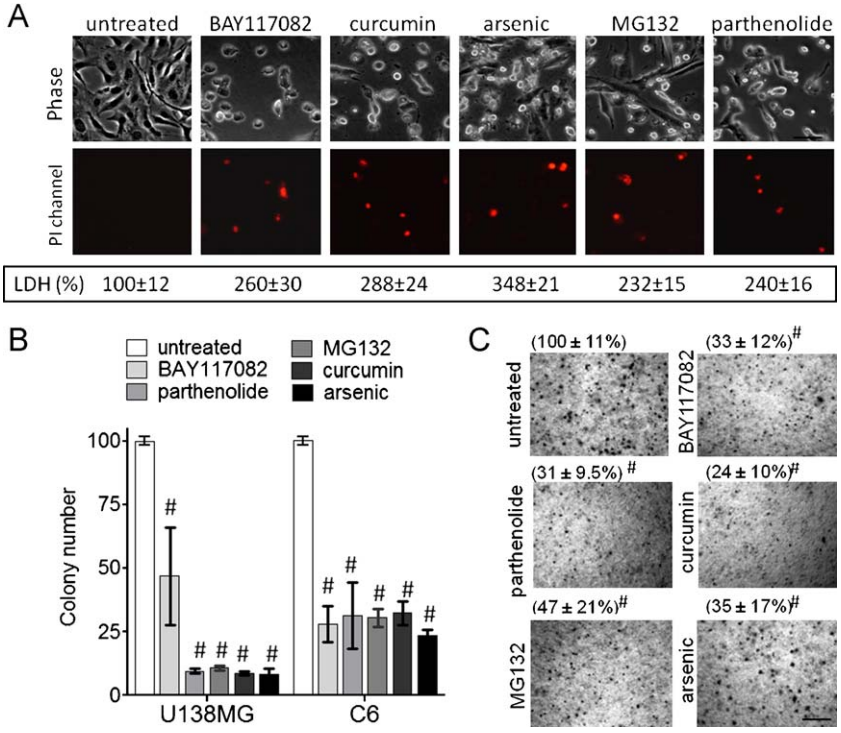

Fig. 4. NFκB inhibitors induce anchorage-independent cell death and reduce clonogenic potential of GBMs. (A) Representative microphotographs (20× magnification) showing cell morphology and PI uptake in U138MG cells after 36 h treatment with NFκB inhibitors. Below microphotographs are presented as means ± SD of the LDH activity detected in the culture medium of GBMs. (B) Clonogenic survival in U138MG cells after treatment with NFκB inhibitors. (C) Representative microphotographs and quantification of colonies in soft agar growing C6 cells (see details in Section 2). In these experiments were used IC_{50} concentrations of NFκB inhibitors. #Different from untreated cells ($n = 3$).

cell death. Like observed in p65 knockdown experiments (Fig. 1), pharmacological inhibitors also decreased the levels of the NFκB-regulated mitochondrial cytoprotective protein bcl-xL [7,10,11] (Fig. 6B). Mitochondrial dysfunction also was accompanied by the release of the pro-apoptotic factor cytochrome c from mitochondrial to cytoplasmic fraction as assessed after 16 h treatment with NFκB inhibitors (Fig. 6B).

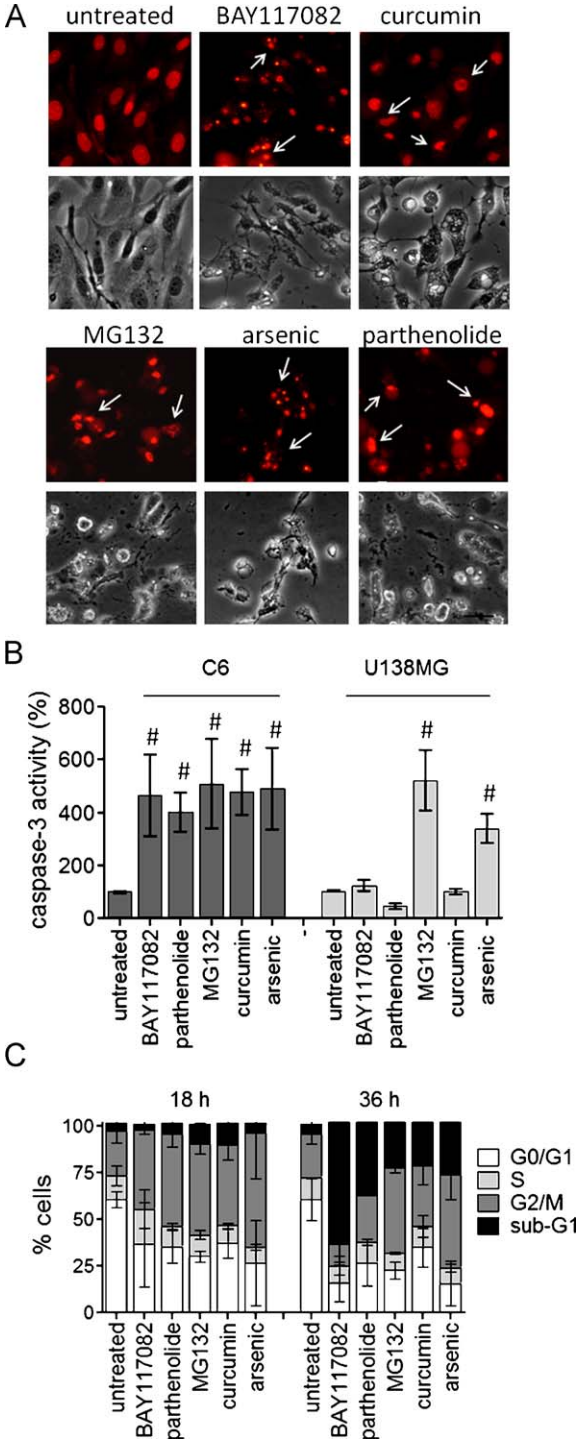

Fig. 5. NFκB inhibitors induce apoptosis in GBMs. (A) Representative fluorescent and phase contrast microphotographs (20×) showing chromatin condensation and apoptotic body formation after 36 h incubation with NFκB inhibitors. U138MG cells were fixed, and chromatin was stained with propidium iodide. (B) Caspase-3 protease activity after 36 h treatment with pharmacological inhibitors in C6 and U138MG cell lines. (C) Quantification of cell population distribution between sub-G1, G1/G0, S and G2/M phases of the cell cycle after 18 or 36 h treatment of U138MG cells with NFκB inhibitors. In Fig. 7 experiments, NFκB inhibitors were incubated using IC_{50} concentrations. #Different from untreated cells ($n = 3$, $p < 0.05$, ANOVA).

3.9. NFκB inhibitors synergize with the anticancer drugs cisplatin and doxorubicin

An interesting field in the NFκB research is the possibility of combination of NFκB inhibitors with classical chemotherapy in order to decrease chemotherapy doses and adverse cytotoxicity to normal tissues [9]. In synergism/antagonism experiments, we established two protocols: (1) 6 h pre-treatment with apoptotic levels of NFκB inhibitors, washout, and 48 h mono-treatment with doxorubicin or cisplatin; (2) 6 h pre-treatment with sub-apoptotic concentrations of NFκB inhibitors followed by 48 h co-incubation with doxorubicin or cisplatin. At the end of the treatments, MTT assays were performed. Results showed that NFκB inhibitors synergized with doxorubicin and cisplatin in both apoptotic and sub-apoptotic concentrations potentiating the anticancer effects of these drugs in C6 and U138MG lines (Table 6).

3.10. NFκB inhibitors overcame cisplatin resistance in GBM

In other approach, we selected cisplatin-resistant cells by incubating C6 cells with 50 μM cisplatin for 48 h followed by a 20–

Table 6
NFκB inhibitors synergize with cisplatin and doxorubicin to induce GBM cell death.

Treatments	Viability (mean ± SD)	
	C6	U138MG
Untreated	100 ± 6	100 ± 7
Cisplatin 5 μM	73 ± 3*	84 ± 8*
Cisplatin + BAY 7.5 μM	55 ± 12#	64 ± 8#
Cisplatin + BAY 25 μM	19 ± 5#	34 ± 16#
Cisplatin + Part 10 μM	56 ± 4#	74 ± 6
Cisplatin + Part 25 μM	38 ± 11#	22 ± 4#
Cisplatin + MG132 1 μM	60 ± 14	68 ± 4#
Cisplatin + MG132 5 μM	33 ± 10#	23 ± 1#
Cisplatin + curcumin 10 μM	46 ± 6#	47 ± 13#
Cisplatin + curcumin 25 μM	36 ± 5#	28 ± 2#
Cisplatin + arsenic 0.5 μM	51 ± 10#	56 ± 1#
Cisplatin + arsenic 15 μM	29 ± 9#	25 ± 3#
Doxorubicin 2.5 μM	70 ± 8*	75 ± 7*
Doxorubicin + BAY 7.5 μM	24 ± 12#	61 ± 6.5
Doxorubicin + BAY 25 μM	21 ± 12#	29 ± 10#
Doxorubicin + Part 10 μM	46 ± 11#	23 ± 5#
Doxorubicin + Part 25 μM	23 ± 2#	19 ± 1#
Doxorubicin + MG132 1 μM	32 ± 7#	22 ± 18#
Doxorubicin + MG132 5 μM	7 ± 1#	2 ± 3#
Doxorubicin + curcumin 10 μM	67 ± 5	59 ± 2#
Doxorubicin + curcumin 25 μM	46 ± 5#	39 ± 3#
Doxorubicin + arsenic 0.5 μM	61 ± 6	25 ± 2#
Doxorubicin + arsenic 15 μM	30 ± 5#	25 ± 1#
BAY 7.5 μM	102 ± 13	103 ± 10
BAY 25 μM	37 ± 5*	53 ± 12*
Part 10 μM	92 ± 9	90 ± 7
Part 25 μM	58 ± 13*	45 ± 13*
MG132 1 μM	114 ± 8	82 ± 10*
MG132 5 μM	77 ± 11*	28 ± 4*
Curcumin 10 μM	94 ± 7	74 ± 12*
Curcumin 25 μM	75 ± 17*	53 ± 11*
Arsenic 0.5 μM	110 ± 18	90 ± 12
Arsenic 15 μM	58 ± 11*	49 ± 10*

Wild-type U138MG and C6 glioma cell lines were treated with different concentrations of NFκB inhibitors as described in Section 3, followed by exposure to 5 μM cisplatin or 2.5 μM doxorubicin (approximately IC_{25} levels) for 48 h. After that, MTT assays were performed. Data were expressed as percentage compared to untreated cells (mean ± SD). Experiments were repeated three times ($n = 3$) in quadruplicate. BAY (BAY117082); Part (Parthenolide).

* Different from untreated cells.

Different from untreated and from cisplatin or doxorubicin-treated cells ($p < 0.05$).

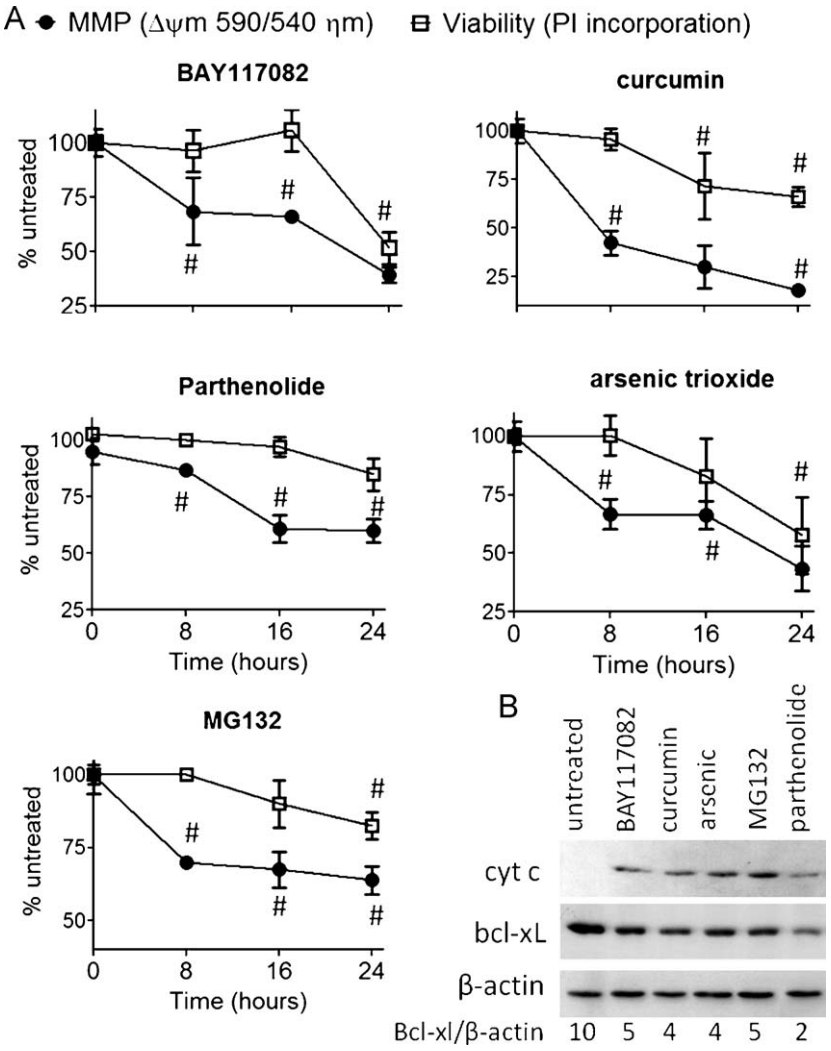

Fig. 6. Mitochondrial dysfunction precedes apoptosis in NFκB inhibitor-treated cells. (A) Time course effect of NFκB inhibitors on MMP was co-evaluated with PI incorporation for the determination of cell membrane integrity. U138MG was treated for different times and, at the end of treatments, cells were trypsinized and different aliquots were assayed by JC-1 or PI incorporation. (B) Western blotting detection of cytochrome c in the cytosolic fraction, and total bcl-xL protein levels in U138MG cells after 16 h treatment with NFκB inhibitors. Experiments were performed in triplicate, and graphs were expressed in mean ± SD. #Different from untreated cells.

25 day washout for the recovery of survival clones. After that, cells were tested for cisplatin resistance. IC_{50} values increased by almost 8-fold (from 20 to 155 μM) confirming the resistance to the alkylating agent (Fig. 7A). Interestingly, NFκB was found over-stimulated in cisplatin-resistant cells compared to wild-type C6 (Fig. 7B). The antiglioma potential of NFκB inhibitors was independent of cisplatin resistance, since drugs were effective to induce cell death in the cisplatin-resistant C6 cell line. Interestingly, co-treatment of cisplatin (IC_{25} concentration = 75 μM) plus NFκB inhibitors overcame cisplatin resistance, finally inducing high rates of cell death after 48 h treatment when compared to mono-treatments of NFκB inhibitors or cisplatin (Fig. 7C). Altogether, data showed that increased NFκB correlated with cisplatin resistance, and NFκB inhibitors efficiently induced cell death in resistant cells besides overcoming cisplatin resistance. Importantly, cell resistance to cisplatin was transitory and decreased after 3–4 passages.

4. Discussion

GBMs are associated with a poor prognosis due to intrinsic malignance and drug/radiation resistance, besides limited therapeutic opportunities such as neurosurgery and temozolomide/radiotherapy regimens [1,15,25]. Studies reported that NFκB activation correlates with therapeutic implications and worse prognosis in human gliomas [21–23,37–39]. Aberrant NFκB activity was found critical for focal necrosis formation, invasive phenotype establishment [22] and resistance to O^6 alkylating agents in GBMs [40]. In vitro, the expression of an IκB super-repressor protein decreased C6 cell viability [21]. Also, the literature indicates that most of the factors that mediate proliferation, invasion, angiogenesis and apoptotic resistance in cancer, including GBMs, such as EGF/EGFR, VEGF, PDGF, MCP-1, MMPs, VCAM, bcl-xL and FLICE are activators of or products of NFκB-regulated genes, conferring to NFκB a potential role on GBM growth and thus a potential target pathway [7,8,11,41,42]. In this way, some experimental drugs possessing antiglioma activities showed mechanisms involving NFκB inhibition [43–46].

In this work, knockdown of the NFκB member p65 and pharmacological inhibition of NFκB caused significant decreases in GBM cell viability whereas inhibitors of other signaling pathways such as MEK/ERK, JNK, p38, EGFR and PKC had no significant effects, except for a cytostatic activity following PI3K/Akt inhibition. Corroborating, Carapancea et al. showed that inhibitors of PDGF, EGFR, PI3K and MEK1/2 (AG1433, AG1024, LY294002 and PD98059, respectively) failed to induce cell death in MO59J and

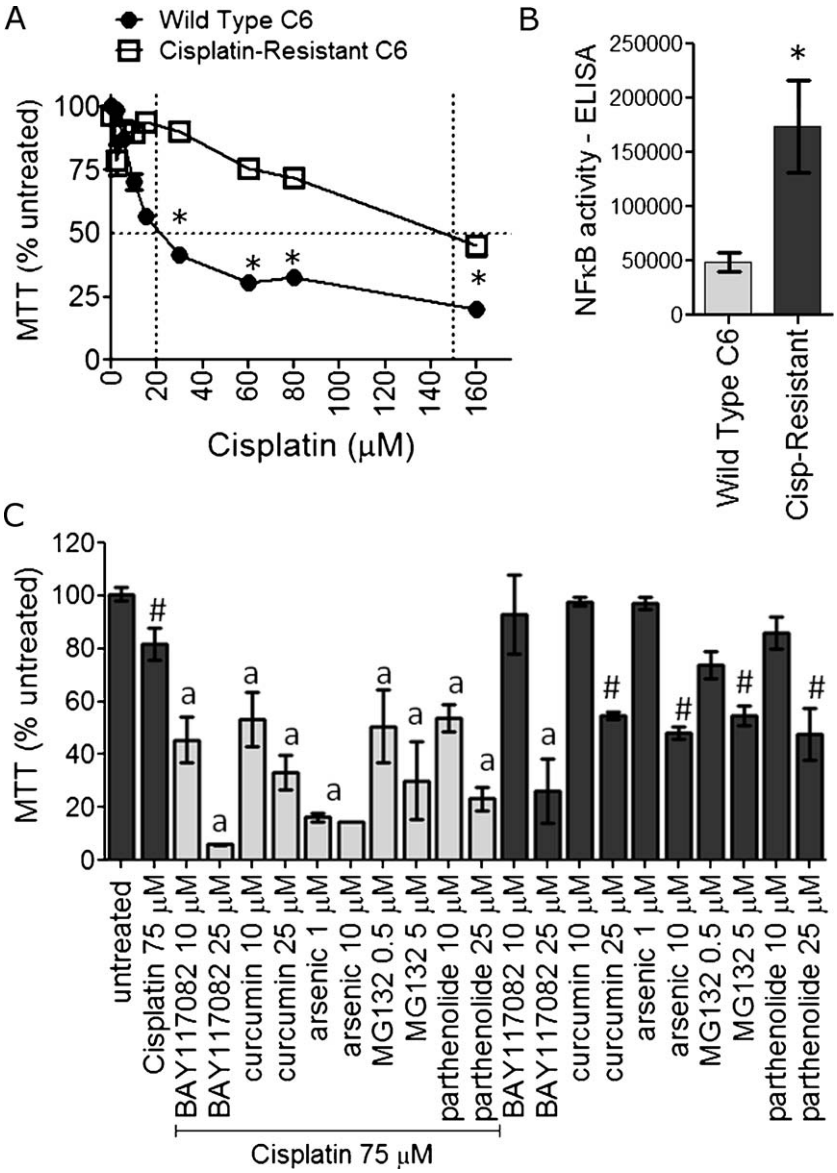

Fig. 7. NFκB inhibitors overcame cisplatin resistance GBM cells. (A) Representative MTT assay showing the validation of cisplatin resistance in C6 cells. (B) NFκB ELISA assay showing that NFκB DNA-binding activity is increased in cisplatin-resistant compared to that of wild-type C6 cells. (C) NFκB inhibition abolishes cisplatin resistance in cisplatin-resistant cells. Cells were treated with IC_{25} concentrations of cisplatin in the presence or absence of NFκB inhibitors (IC_{50} levels) for 48 h, and viability was determined by MTT. Resistance induction was performed twice, and experiments were performed in triplicate. *Different from C6-wild type cells; #different from untreated cells; [a]different from cisplatin and from its respective NFκB inhibitor alone treatment.

MO59K cell lines, and in primary cultures derived from GBM patients [47]. NFκB inhibitors induced cell death in liquid and soft agar growing cells regardless of the p53 or PTEN mutational status since cytotoxicity was similar for C6 (p53 and PTEN normal), U87 (PTEN mutant), U373 (p53 and PTEN mutant) and U138MG (p53 and PTEN mutant) cell lines. NFκB was found overstimulated in GBMs, and its inhibitors were selective to cell death induction in tumor cells as compared to astrocytes. The antiglioma potential of the pharmacological agents correlated with NFκB inhibition as demonstrated in Tables 4 and 5. Tumor-specific targeting represents an improvement over classical chemotherapeutics, which adversely affect both diseased and normal brain in a non-specific manner [6,9,13]. Nuclear p65 was found in GBMs whereas latent/cytosolic p65 was detected in astrocytes. Total p65 protein was similar between GBM and astrocytes suggesting that NFκB was modulated at the level of activation. Nonetheless, landscapes analysis for NFκB gene interaction network revealed that NFκB target genes were up-regulated in the three tumor grades (GBM, oligodendroglioma and astrocytoma) compared to healthy brain tissues. Landscapes evidenced a high expression of NFκB target genes in the most aggressive form of glioma, GBM; marked increases were observed in VEGFA, MMP2, MMP9, PLAU, VCAM1, ICAM1, IER3, SOD2, MYC, CCL2 and IL8 gene expression. In agreement with these results, Xie et al. showed that constitutive NFκB regulates the expression of VEGF and IL-8 and tumor angiogenesis in human GBM [12]. This exacerbated activation of NFκB has been pivotal to explain the selective toxicity of NFκB inhibitors to cancer cells [10,13,17,19].

Previous works showed that downregulation of NFκB leads to mitochondrial dysfunction due to decreases in the expression of mitochondrial cytoprotective genes such as bcl-xL and SOD2, which result in cytotoxicity [11,15,17,26]. Jiang et al. reported that selective bcl-xL knockdown rendered U87 and NS008 GBM cells to apoptosis [48]. In our model, NFκB inhibitors caused bcl-xL protein downregulation, mitochondrial depolarization and release of the apoptotic factor cytochrome c, which preceded the losses in cell

membrane integrity and apoptosis, thus implying that mitochondrial dysfunction is an early step of NFκB inhibitor-induced cell death [7,11,15,48]. In previous studies, arsenic trioxide induced G2/M arrest in the U87 and T98G [49], and mitochondrial aggregation and cytochrome c release in A172 GBMs [50]. Here, all NFκB inhibitors elicited cell arrest in the G2/M phase of the cell cycle before sub-G1 induction, apoptotic body formation and caspase-3 activation. The herein reported impairment on mitochondrial function and induction of G2/M arrest were previously demonstrated by our group and others during curcumin [51], parthenolide [52], BAY117082 and MG132 [17] treatment in other types of cancer cells, but not in gliomas.

In GBMs, defects in caspase-mediated apoptotic signaling due to p53 mutations limit the effectiveness of chemotherapy thus promoting chemoresistance and poor clinical outcome [53–56]. Induction of caspase-independent mechanisms of cell death could be useful for circumventing GBM resistance. In our model, all tested NFκB inhibitors activated caspase-3 in C6 whereas only MG132, arsenic trioxide and p65 siRNA stimulated caspase-3 in the p53-mutant U138MG; curcumin, BAY117082 and parthenolide exerted caspase-independent cell death in U138MG. Besides the distinct genetic aberrations between C6 and U138MG cell lines, differences in the action mechanisms of the tested NFκB inhibitors and possible off-target effects could explain their differential effects upon caspase-3. BAY117082 is a specific IKK-beta inhibitor ($IC_{50} \sim 10\ \mu M$) [57]; parthenolide inhibits NF-κB both indirectly by blocking IKK-beta at cys179 and directly by inhibiting p65 at the cysteine residue in its activation loop ($IC_{50} \sim 10\ \mu M$) [58,59]; MG132 inhibits proteasome ($IC_{50} \sim 0.1\ \mu M$) and proteasome-dependent IκB-alpha degradation ($IC_{50} \sim 3\ \mu M$) thus blocking the nuclear activity of NFκB; arsenic trioxide inhibits degradation and up-regulates expression of IκB-alpha [60]; curcumin inhibits IKKs ($IC_{50} \sim 13\ \mu M$), although unspecific effects upon activator protein-1 and glyoxalase I activity, for example, were described [15,61,62]. In U138MG, the IKK inhibitors did not increase caspase-3 in contrast to inhibitors of IκB degradation such as MG132 and arsenic. In T98G and U87 GBMs, curcumin induces caspase- and calpain-independent cell death irrespective of the p53 status of the cells [15]. Thus, elucidation of these mechanistic differences requires further investigation.

Besides their apoptotic activity per se, NFκB inhibitors presented adjuvant activity by potentiating the anticancer effect of cisplatin and doxorubicin in both C6 and U138MG cells, besides overcoming cisplatin resistance in cisplatin-resistant C6. Several lines of evidence suggest NFκB as a key mediator of cancer cells resistance to chemotherapy and anticancer therapy failure in vivo [9,18,40]. Bredel et al. reported that NFκB mediates GBM resistance to the alkylating agents, temozolomide and BCNU, in primary GBM cultures [40]. In addition, Weaver et al. demonstrated that chemotherapy-induced DNA damage may activate NFκB, and inhibition of NFκB by mutant IκB-alpha enhances BCNU, carboplatin and TNF-induced cell death in U87 and U251 cells [63]. In our model, NFκB activity was up-regulated in cisplatin-resistant C6 cells compared to that in wild-type C6. Cisplatin-resistant cells remained sensitive to NFκB inhibitors, and combination of cisplatin plus NFκB inhibitors overcame cisplatin resistance, suggesting that alkylation resistance involved NFκB pathway. In agreement, previous studies reported that the proteasome inhibitors LLnL and MG132, which are known by acting through NFκB inhibition, sensitized GBMs to TRAIL-induced apoptosis [18]. Clinically, the adjuvant potential of NFκB inhibitors could be used for therapeutic advantage in order to potentiate the efficacy of classical anticancer drugs in chemotherapy-resistant patients thus decreasing the anticancer agents' doses and the frequently observed collateral effects to healthy tissues [9,15].

As above cited, some previous studies exploited the antiglioma effects of some of the herein used compounds as arsenic trioxide [49,50,64], curcumin [15,65–67], parthenolide [68] and proteasome/NFκB inhibitors [3,18,63,69,70] in GBMs. Here, we suggest that a mechanism by which they induce GBM cells death is mediated by their NFκB inhibitory activity. We add information by evaluating inhibitors of different signaling pathways, NFκB pathway activation in cell lines and in clinical specimens, and effect of different NFκB inhibitors in a panel of GBM cell lines; p65 knockdown also was evaluated. Importantly, selectivity to cancer cells, mitochondrial dysfunction, adjuvant potential and ability of NFκB inhibitors to abolish chemoresistance were examined. The results were positive and support a rationale for further testing inhibition of NFκB pathway in animal models of GBMs, and possibly other cancers.

Disclosure statement

The authors report no conflicts of interest. The authors alone are responsible for the content and writing of the paper.

Acknowledgements

We acknowledge the Brazilian funds CAPES, FINEP/IBNNet (01060842-00) and CNPq for financial support, and Dr Rafael Roesler (Hospital de Clinicas de Porto Alegre, HCPA) for kindly providing U87 and U373 cell lines.

References

[1] Stewart LA. Chemotherapy in adult high-grade glioma: a systematic review and meta-analysis of individual patient data from 12 randomised trials. Lancet 2002;359:1011–8.
[2] Soni D, King JA, Kaye AH, Hovens CM. Genetics of glioblastoma multiforme: mitogenic signaling and cell cycle pathways converge. J Clin Neurosci 2005;12:1–5.
[3] Yu C, Friday BB, Yang L, Atadja P, Wigle D, Sarkaria J, et al. Mitochondrial Bax translocation partially mediates synergistic cytotoxicity between histone deacetylase inhibitors and proteasome inhibitors in glioma cells. Neuro Oncol 2008;10(3):309–19.
[4] Brennan C, Momota H, Hambardzumyan D, Ozawa T, Tandon A, Pedraza A, et al. Glioblastoma subclasses can be defined by activity among signal transduction pathways and associated genomic alterations. PLoS ONE 2009; 4(11):e7752.
[5] Gerstner ER, Sorensen AG, Jain RK, Batchelor TT. Anti-vascular endothelial growth factor therapy for malignant glioma. Curr Neurol Neurosci Rep 2009;9(3):254–62.
[6] Mercer RW, Tyler MA, Ulasov IV, Lesniak MS. Targeted therapies for malignant glioma: progress and potential. BioDrugs 2009;23(1):25–35.
[7] Barkett M, Gilmore TD. Control of apoptosis by Rel/NFkB transcription factors. Oncogene 1999;18:6910–24.
[8] Rayet B, Gélinas C. Aberrant rel/NFκB genes and activity in human cancer. Oncogene 1999;18(49):6938–47.
[9] Nakanishi C, Toi M. Nuclear factor-kappaB inhibitors as sensitizers to anticancer drugs. Nat Rev Cancer 2005;5(4):297–309.
[10] Baud V, Karin M. Is NF-kB a good target for cancer therapy? Hopes and pitfalls. Nat Rev Drug Discov 2009;8:33–40.
[11] Aggarwal BB. Nuclear factor-kappaB: the enemy within. Cancer Cell 2004;6(3):203–8.
[12] Xie TX, Xia Z, Zhang N, Gong W, Huang S. Constitutive NF-kappaB activity regulates the expression of VEGF and IL-8 and tumor angiogenesis of human glioblastoma. Oncol Rep 2010;23(3):725–32.
[13] Orlowski RZ, Baldwin Jr AS. NF-kappa B as a therapeutic target in cancer. Trends Mol Med 2002;8:385–9.
[14] Li B, Li YY, Tsao SW, Cheung AL. Targeting NF-kappaB signaling pathway suppresses tumor growth, angiogenesis, and metastasis of human esophageal cancer. Mol Cancer Ther 2009;8(9):2635–44.
[15] Dhandapani KM, Mahesh VB, Brann DWJ. Curcumin suppresses growth and chemoresistance of human glioblastoma cells via AP-1 and NFkappaB transcription factors. J Neurochem 2007;102(2):522–38.
[16] Xie TX, Aldape KD, Gong W, Kanzawa T, Suki D, Kondo S, et al. NF-kappaB activity is critical in focal necrosis formation of human glioblastoma by regulation of the expression of tissue factor. Int J Oncol 2008;33(1):5–15.
[17] Zanotto-Filho A, Delgado-Cañedo A, Schröder R, Becker M, Klamt F, Moreira JC. The pharmacological NFkappaB inhibitors BAY117082 and MG132 induce cell arrest and apoptosis in leukemia cells through ROS–mitochondria pathway activation. Cancer Lett 2010;288(2):192–3.

[18] Kasuga C, Ebata T, Kayagaki N, Yagita H, Hishii M, Arai H, et al. Sensitization of human glioblastomas to tumor necrosis factor-related apoptosis-inducing ligand (TRAIL) by NF-kappaB inhibitors. Cancer Sci 2004;95(10):840–4.
[19] Pickering BM, de Mel S, Lee M, Howell M, Habens F, Dallman CL, et al. Pharmacological inhibitors of NF-kB accelerate apoptosis in chronic lymphocytic leukemia cells. Oncogene 2007;26:1166–77.
[20] Domingo-Domènech J, Pippa R, Tápia M, Gascón P, Bachs O, Bosch M. Inactivation of NF-kappaB by proteasome inhibition contributes to increased apoptosis induced by histone deacetylase inhibitors in human breast cancer cells. Breast Cancer Res Treat 2008;112(1):53–62.
[21] Robe PA, Bentires-Alj M, Bonif M, Rogister B, Deprez M, Haddada H, et al. In vitro and in vivo activity of the nuclear factor-kappaB inhibitor sulfasalazine in human glioblastomas. Clin Cancer Res 2004;10(16):5595–603.
[22] Raychaudhuri B, Han Y, Lu T, Vogelbaum MA. Aberrant constitutive activation of nuclear factor kappaB in glioblastoma multiforme drives invasive phenotype. J Neurooncol 2007;85(1):39–47.
[23] Brown RE, Law A. Morphoproteomic demonstration of constitutive nuclear factor-kappaB activation in glioblastoma multiforme with genomic correlates and therapeutic implications. Ann Clin Lab Sci 2006;36(4):421–6.
[24] da Frota Jr ML, Braganhol E, Canedo AD, Klamt F, Apel MA, Mothes B, et al. Brazilian marine sponge Polymastia janeirensis induces apoptotic cell death in human U138MG glioma cell line, but not in a normal cell culture. Invest New Drugs 2009;27(1):13–20.
[25] Braganhol E, Zamin LL, Cañedo AD, Horn F, Tamajusuku AS, Wink MR, et al. Antiproliferative effect of quercetin in the human U138MG glioma cell line. Anticancer Drugs 2006;17(6):663–71.
[26] Zanotto-Filho A, Gelain DP, Schröder R, Souza LF, Pasquali MA, Klamt F, et al. The NFkappaB-mediated control of RS and JNK signaling in vitamin A-treated cells: duration of JNK–AP-1 pathway activation may determine cell death or proliferation. Biochem Pharmacol 2009;77:1291–301.
[27] Bharti AC, Donato N, Singh S, Aggarwal BB. Curcumin (diferuloylmethane) down-regulates the constitutive activation of nuclear factor-kappa B and IkappaBalpha kinase in human multiple myeloma cells, leading to suppression of proliferation and induction of apoptosis. Blood 2003;101(3):1053–62.
[28] Klamt F, Shacter E. Taurine chloramine, an oxidant derived from neutrophils, induces apoptosis in human B lymphoma cells through mitochondrial damage. J Biol Chem 2005;280:21346–52.
[29] Hirose Y, Berger MS, Pieper RO. p53 affects both the duration of G2/M arrest and the fate of temozolomide-treated human glioblastoma cells. Cancer Res 2001;61:1957–63.
[30] Kucharczak J, Simmons MJ, Fan Y, Gélinas C. To be, or not to be: NF-kappaB is the answer: role of Rel/NF-kappaB in the regulation of apoptosis. Oncogene 2003;22(56):8961–82.
[31] Kim HJ, Hawke N, Baldwin AS. NF-kappaB and IKK as therapeutic targets in cancer. Cell Death Differ 2006;13(5):738–47.
[32] von Mering C, Jensen LJ, Snel B, Hooper SD, Krupp M, Foglierini M, et al. STRING: known and predicted protein–protein associations, integrated and transferred across organisms. Nucleic Acids Res 2005;33:433–7.
[33] Wain HM, Lush MJ, Ducluzeau F, Khodiyar VK, Povey S. Genew: the Human Gene Nomenclature Database, 2004 updates. Nucleic Acids Res 2004;32:255–7.
[34] Birney E, Andrews D, Caccamo M, Chen Y, Clarke L, Coates G, et al. Ensembl 2006. Nucleic Acids Res 2006;34:556–61.
[35] Hooper SD, Bork P. Medusa: a simple tool for interaction graph analysis. Bioinformatics 2005;21:4432–3.
[36] Castro MAA, Rybarczyk Filho JL, Dalmolin RJS, Sinigaglia M, Moreira JCF, Mombach JCM, et al. ViaComplex: software for landscape analysis of gene expression networks in genomic context. Bioinformatics 2009;25(11):1468–9.
[37] Park S, Hatanpaa KJ, Xie Y, Mickey BE, Madden CJ, Raisanen JM, et al. The receptor interacting protein 1 inhibits p53 induction through NF-kappaB activation and confers a worse prognosis in glioblastoma. Cancer Res 2009;69(7):2809–16.
[38] Park S, Zhao D, Hatanpaa KJ, Mickey BE, Saha D, Boothman DA, et al. RIP1 activates PI3K–Akt via a dual mechanism involving NF-kappaB-mediated inhibition of the mTOR–S6K–IRS1 negative feedback loop and down-regulation of PTEN. Cancer Res 2009;69(10):4107–11.
[39] Wang H, Wang H, Zhang W, Huang HJ, Liao WS, Fuller GN. Analysis of the activation status of Akt, NFkappaB, and Stat3 in human diffuse gliomas. Lab Invest 2004;84(8):941–51.
[40] Bredel M, Bredel C, Juric D, Duran GE, Yu RX, Harsh GR, et al. Tumor necrosis factor-alpha-induced protein 3 as a putative regulator of nuclear factor-kappaB-mediated resistance to O^6-alkylating agents in human glioblastomas. J Clin Oncol 2006;24(2):274–87.
[41] Kapoor GS, Zhan Y, Johnson GR, O'Rourke DM. Distinct domains in the SHP-2 phosphatase differentially regulate epidermal growth factor receptor/NF-kappaB activation through Gab1 in glioblastoma cells. Mol Cell Biol 2004;24(2):823–36.
[42] Sethi G, Ahn KS, Chaturvedi MM, Aggarwal BB. Epidermal growth factor (EGF) activates nuclear factor-kappaB through IkappaBalpha kinase-independent but EGF receptor-kinase dependent tyrosine 42 phosphorylation of Ikappa-Balpha. Oncogene 2007;26(52):7324–32.
[43] Gao X, Deeb D, Jiang H, Liu Y, Dulchavsky SA, Gautam SC. Synthetic triterpenoids inhibit growth and induce apoptosis in human glioblastoma and neuroblastoma cells through inhibition of prosurvival Akt, NF-kappaB and Notch1 signaling. J Neurooncol 2007;84(2):147–57.
[44] Kotliarova S, Pastorino S, Kovell LC, Kotliarov Y, Song H, Zhang W, et al. Glycogen synthase kinase-3 inhibition induces glioma cell death through c-MYC, nuclear factor-kappaB, and glucose regulation. Cancer Res 2008;68(16):6643–51.
[45] Sharma V, Tewari R, Sk UH, Joseph C, Sen E. Ebselen sensitizes glioblastoma cells to Tumor Necrosis Factor (TNFalpha)-induced apoptosis through two distinct pathways involving NF-kappaB downregulation and Fas-mediated formation of death inducing signaling complex. Int J Cancer 2008;123(9):2204–12.
[46] Kuwayama K, Matsuzaki K, Mizobuchi Y, Mure H, Kitazato KT, Kageji T, et al. Promyelocytic leukemia protein induces apoptosis due to caspase-8 activation via the repression of NFkappaB activation in glioblastoma. Neuro Oncol 2009;11(2):132–41.
[47] Carapancea M, Alexandru O, Fetea AS, Dragutescu L, Castro J, Georgescu A, et al. Growth factor receptors signaling in glioblastoma cells: therapeutic implications. Neurooncology 2009;92(2):137–47.
[48] Jiang Z, Zheng X, Rich KM. Down-regulation of Bcl-2 and Bcl-xL expression with bispecific antisense treatment in glioblastoma cell lines induce cell death. J Neurochem 2003;84:273–81.
[49] Zhao S, Tsuchida T, Kawakami K, Shi C, Kawamoto K. Effect of As_2O_3 on cell cycle progression and cyclins D1 and B1 expression in two glioblastoma cell lines differing in p53 status. Int J Oncol 2002;21(1):49–55.
[50] Haga N, Fujita N, Tsuruo T. Involvement of mitochondrial aggregation in arsenic trioxide (As_2O_3)-induced apoptosis in human glioblastoma cells. Cancer Sci 2005;96(11):825–33.
[51] Chiu TL, Su CC. Curcumin inhibits proliferation and migration by increasing the Bax to Bcl-2 ratio and decreasing NF-kappaB p65 expression in breast cancer MDA-MB-231 cells. Int J Mol Med 2009;23(4):469–75.
[52] Hayashi S, Sakurai H, Hayashi A, Tanaka Y, Hatashita M, Shioura H. Inhibition of NF-kappaB by combination therapy with parthenolide and hyperthermia and kinetics of apoptosis induction and cell cycle arrest in human lung adenocarcinoma cells. Int J Mol Med 2010;25(1):81–7.
[53] Sidransky D, Mikkelsen T, Schwechheimer K, Rosenblum ML, Cavanee W, Vogelstein B. Clonal expansion of p53 mutant cells is associated with brain tumour progression. Nature 1992;355:846–7.
[54] Lowe SW, Bodis S, McClatchey A, Remington L, Ruley HE, Fisher DE, et al. p53 status and the efficacy of cancer therapy in vivo. Science 1994;266:807–10.
[55] Lowe SW, Ruley HE, Jacks T, Housman DE. p53-dependent apoptosis modulates the cytotoxicity of anticancer agents. Cell 1993;74:957–67.
[56] Igney FH, Krammer PH. Death and anti-death: tumour resistance to apoptosis. Nat Rev Cancer 2002;2:277–88.
[57] Pierce JW, Schoenleber R, Jesmok G, Best J, Moore SA, Collins T, et al. Novel inhibitors of cytokine-induced IκBα phosphorylation and endothelial cell adhesion molecule expression show anti-inflammatory effects in vivo. J Biol Chem 1997;272:21096–103.
[58] Kwok BH, Koh B, Ndubuisi MI, Elofsson M, Crews CM. The anti-inflammatory natural product parthenolide from the medicinal herb Feverfew directly binds to and inhibits IκB kinase. Chem Biol 2001;8:759–66.
[59] Hehner SP, Hofmann TG, Droge W, Schmitz ML. The antiinflammatory sesquiterpene lactone parthenolide inhibits NF-κB by targeting the IκB kinase complex. J Immunol 1999;163:5617–23.
[60] Han SS, Kim K, Hahm ER, Park CH, Kimler BF, Lee SJ, et al. Arsenic trioxide represses constitutive activation of NF-kappaB and COX-2 expression in human acute myeloid leukemia, HL-60. J Cell Biochem 2005;94:695–7.
[61] Kasinski AL, Du Y, Thomas SL, Zhao J, Sun SY, Khuri FR, et al. Inhibition of IkappaB kinase–nuclear factor-kappaB signaling pathway by 3,5-bis(2-flurobenzylidene)piperidin-4-one (EF24), a novel monoketone analog of curcumin. Mol Pharmacol 2008;74:654–61.
[62] Santel T, Pflug G, Hemdan NY, Schäfer A, Hollenbach M, Buchold M, et al. Curcumin inhibits glyoxalase 1: a possible link to its anti-inflammatory and anti-tumor activity. PLoS ONE 2008;3(10):e3508.
[63] Weaver KD, Yeyeodu S, Cusack Jr JC, Baldwin Jr AS, Ewend MG. Potentiation of chemotherapeutic agents following antagonism of nuclear factor kappa B in human gliomas. J Neurooncol 2003;61:187–96.
[64] Pucer A, Castino R, Mirković B, Falnoga I, Slejkovec Z, Isidoro C, et al. Differential role of cathepsins B and L in autophagy-associated cell death induced by arsenic trioxide in U87 human glioblastoma cells. Biol Chem 2010;391(5):519–31.
[65] Perry MC, Demeule M, Régina A, Moumdjian R, Béliveau R. Curcumin inhibits tumor growth and angiogenesis in glioblastoma xenografts. Mol Nutr Food Res 2010;54(8):1192–201.
[66] Karmakar S, Banik NL, Ray SK. Curcumin suppressed anti-apoptotic signals and activated cysteine proteases for apoptosis in human malignant glioblastoma U87MG cells. Neurochem Res 2007;32(12):2103–13.
[67] Liu E, Wu J, Cao W, Zhang J, Liu W, Jiang X, et al. Curcumin induces G2/M cell cycle arrest in a p53-dependent manner and upregulates ING4 expression in human glioma. J Neurooncol 2007;85(3):263–70.
[68] Anderson KN, Bejcek BE. Parthenolide induces apoptosis in glioblastomas without affecting NF-kappaB. J Pharmacol Sci 2008;106(2):318–20.
[69] Wagenknecht B, Hermisson M, Groscurth P, Liston P, Krammer PH, Weller M. Proteasome inhibitor-induced apoptosis of glioma cells involves the processing of multiple caspases and cytochrome c release. J Neurochem 2000;75(6):2288–97.
[70] Wagenknecht B, Hermisson M, Eitel K, Weller M. Proteasome inhibitors induce p53/p21-independent apoptosis in human glioma cells. Cell Physiol Biochem 1999;9(3):117–25.